3D Human Posture Segmentation by Constrained Spectral Clustering

Jun Cheng[a,b], Maoying Qiao[a,b], Wei Bian[c], Dacheng Tao[c]

[a] *Shenzhen Institutes of Advanced Technology, Chinese Academy of Sciences, China*
[b] *The Chinese University of Hong Kong, Hong Kong, China*
[c] *Centre for Quantum Computation and Intelligence Systems, University of Technology, Sydney, NSW 2007, Australia*

Abstract

In this paper, we propose a new algorithm for partitioning human posture represented by 3D point clouds sampled from the surface of human body. The algorithm is formed as a constrained extension of the recently developed segmentation method, spectral clustering (SC). Two folds of merits are offered by the algorithm: 1) as a nonlinear method, it is able to deal with the situation that data (point cloud) are sampled from a manifold (the surface of human body) rather than the embedded entire (3D) space; 2) by using constraints, it facilitates the integration of multiple similarities for human posture partitioning, and it also helps to reduce the limitations of spectral clustering. We show that the constrained spectral clustering (CSC) still can be solved by generalized eigen-decomposition. Experimental results confirm the effectiveness of the proposed algorithm.

Keywords: Constrained Spectral Clustering, 3D Human Posture Segmentation.

1. Introduction

3D human point cloud data, recent years, along with emergence of kinds of human body scanners, is becoming usable, so it is being popular used in various applications(Werghi and Xiao, 2002; K.H., 2002). Human behavior analysis is an important task in various applications (Chen et al., 2006; Weik et al., 2001) like human behavior recognition, real-time tracking system, human interaction system, human-machine control system, and so on.

Considering significance of human behavior analysis and novelty of 3D human point cloud data, employing 3D point cloud data into human behavior analysis is an inevitable trend.

A fundamental and important issue in 3D point cloud based human behavior analysis is posture partitioning, i.e., partition the human body into semantic parts, such as, torso and limbs. The partitioning of human posture is valuable to motion estimation and recognition(Song et al., 2003; Mori et al., 2004). By using the obtained clusters, which represent different parts of the human body, we can give a more compact and robust description of motion than using the raw data. Moreover, it also serves as a preprocessing and benefits the high-level tasks afterward, e.g., recognition and tracking of human behavior(Yilmaz et al., 2006). The partitioning of human posture into a small number of semantic parts helps reducing the complexity of the dynamic system of tracking, which is valuable to both improve the accuracy and reduce computation cost.

However,there are several difficulties in partitioning human posture represented by 3D point cloud. First, data from the point cloud are scattered on a 2D manifold of human surface embedded in the 3D space. Due to the utilization of Euclidean distance, classical sum of squared distance method, i.e., k-means(Kanungo et al., 2002), or probability density based method, Gaussian mixture models (GMM)(hsuan Yang and Ahuja, 1999), are unable to find suitable clusters on manifold. Thus, nonlinear approach should be used to integrate geodesic distance between points into the partitioning process so that the manifold structure can be properly addressed. Second, to obtain a partitioning result with reasonably semantic meanings, it is necessary to exploit multiple similarities between the data point on the manifold (human surface), e.g., distance similarity and surface normal similarity. However, the integration of multiple similarities into the partitioning of data point scattered on a manifold is more challenging.

In this paper, we propose a new algorithm, called constrained spectral clustering (CSC), for partitioning the point cloud data of human posture into semantic parts. CSC duly addresses all aforementioned difficulties. On one hand, CSC belongs to the graph-based partitioning algorithm, which only utilizes local similarities between data points, and thus is able to deal with the manifold structure of human surface. On the other hand, CSC formulates extra similarities (could be more than one although we use only one extra similarity in this paper) as constraints for optimization so as to obtain a partitioning results consistent with multiple similarities. We prove

that, like spectral clustering (SC), CSC can also be effectively solved by using eigen-decomposition. Sufficient experiments are performed to evaluate the effectiveness of the proposed algorithm.

The rest of this paper is organized as follows. Section 2 gives a brief review of related works on human posture partitioning and clustering algorithms. Section 3 presents the multiple similarities, i.e., distance similarity and surface normal similarity, used in this paper for human posture partitioning. In Section 4, we derive the proposed algorithm, constrained spectral clustering (CSC). We report experimental results in Section 5. Finally, Section 6 concludes this paper and gives discussions on future works.

2. Related Works

In the past recent years, extensive researches have been done on 3D point cloud data and technology of segmenting human posture formed by 3D point cloud into semantic parts is one of them(Werghi and Xiao, 2002; K.H., 2002; Nurre, 1997; Jagannathan, 2005). But automatic segmentation of human body is a challenging problem which is determined by several reasons. First, the body shape is both articulated and deformable. Second, the point cloud is unorganized.

The pioneer investigated in this area is Nurre (Nurre, 1997). He means to segment the human body into six segments, corresponding to a stick template consisted of head, two arms, two legs, torso, which represents the body structure. He combines a global shape description of moments analysis and local criteria of proximity which are derived from a priori knowledge of the relative positions of the body parts in the standard posture to achieve his task. The data is organized into slices of data points and the data points are assigned to the different body parts according to the slice's topology and its position in the body. Under the framework of Nurre's, several more works are done to improve his results. Ju et al.'s work (Ju et al., 2000)introduces curvature analysis of profiles to allow further decomposition of body limbs into their articulated segments. Dekker and Douros'work (Dekker et al., 1999) improves the localization of the key landmarks of Nurre's work.

Certainly, these works illustrate a considerable progress towards the automatic decomposition of the human body data. However these approaches are only effective in strict standard posture. Besides, there have no evidence of robustness with respect to noise, gaps in the data, and variation in the shape and the posture of the human body. Aiming at these demerits, Xiao et

al. devote themselves to extract global topological features by using discrete reeb graph theory to represent the body shape(Xiao et al., 2003). As their method doesn't involve local feature analysis, as long as the whole structure of the human body does not change, their approach is robust against noise, posture variation. However, all above methods, being based on topological analysis, are intrinsically not qualified to handle postures where limbs are joined together. Wang et al. propose a approach from another perspective that develops within a Fuzzy logic framework(C.C.L et al., 2003). However, the overall performance of this approach remains identical to that of Nurre's.

A novel method for 3D human body point cloud segmentation is proposed in our paper. We achieve our segmentation mission using clustering method. As the 3D data points scatter on a human body manifold, we choose a nonlinear clustering method to obtain considerable results.

3. Multiple Similarities

In this section, we present the distance similarity and the surface normal similarity that are used in our partitioning algorithm.

3.1. Distant Similarity

Without prior knowledge, distance similarity between points is the main information that we can obtain from the 3D point cloud for partitioning. Denoting the collection of all the N points from the point cloud as V, then for any x_i and $x_j \in V$, the Euclidean distance between them is given by

$$dist(i,j) = \|x_i - x_j\|_2 \tag{1}$$

The Euclidean distance defined above is unsuitable to be directly used for partitioning, because the points in V are scattered on a manifold. Within a local area, the Euclidean distance can approach the geodesic distance on the manifold. Thus, we can use the exponential function to emphasize the local Euclidean distance

$$W(i,j) = \exp\{-\frac{dist(i,j)}{\sigma^2}\} \tag{2}$$

where σ is a scale parameter to control the size of the local area. And, we call $W(i,j)$ the distance similarity between x_i and x_j. Note that the N by N matrix W is just the affinity matrix used in SC if we construct a fully connected graph on V and define the weight of each edge by using

(2). Figure. 1(a) gives an illustration of the distance similarity. Five points appearing as dark red centers are taken as examples. Different colored rings where points having the same distance similarity locate on around the center explan different distance similarity. Points on rings that is farthest from center have smallest distance similarity with point on center. And the points who are not on rings have zero degree distance similarity with these centers.

As aforementioned, the distance similarity will be used as the main information in our algorithm CSC for posture portioning. However, if only using the distance similarity distance, we cannot obtain a satisfied partition, because the localized distance similarity does not guarantee to recover globally semantic parts of the human body. This is reflected by the fact that SC tends to partition a large area, which is a single cluster in the semantic meaning, into several small clusters(Kannan et al., 2000). To address this problem, as discussed in the next subsection, we will introduce another similarity, which is used as constraints in our algorithm CSC, to reduce the possibility of partitioning one semantic part into small ones.

3.2. Surface Normal Similarity

Another feature can be used to characterize the similarity between points on a manifold is surface normal. Especially in our study, the points located in the center of semantic parts of human body are likely to have similar surface normal, while the points from different semantic parts generally do not have similar surface normal due to the human body structure and the angles between body parts caused by motions. Figure. 1(b) shows some examples for the surface normal similarity. Upper legs, lower legs and lower arms are not crossing the joints, as their original appearance, they have strip-like surface normal similarities respectively. And as torso is a large flat area, it has square-like surface normal similarities.

Although we want to calculate the surface normal of a point on human body, we do not really fit a surface to the local area around that point since the fitting is generally computationally consuming. Instead, we use a simple way to roughly approximate the surface normal. Given point x from V, we first find its k nearest neighbors $X = [x_1, x_2, ..., x_k]$. Further, principal component analysis (PCA) is used to calculate the minimum variance direction. Specifically, by singular value decomposition, we have

$$\bar{X} = \sum_{i=1}^{3} \lambda_i \xi_i \zeta_i^T, \quad \lambda_1 \geq \lambda_2 \geq \lambda_3 \tag{3}$$

where $\bar{X}$ is centralized X by subtracting the mean vector. Then, we use ξ_3 as the approximate surface normal π of point x.

To further reduce computation cost, we only calculate the surface normal on a randomly sampled small portion $\tilde{V}$ of all the points in V. Given any x_i and $x_j \in V$, we say they have similar surface normal, i.e.,

$$S(i,j) = 1 \tag{4}$$

If they are k nearest neighbor of each other and the angles between their surface normal π_i and π_j is smaller than a threshold, i.e.,$(\pi_i, \pi_j) < \delta$. It is worth emphasizing that the "hard" setting of similarity in (4) rather than the "soft" one in (2). That's because we only use surface normal similarity to formulate constraints but not to use it as the main information for partitioning. Besides, since the surface normal on a large portion of the points in V are not calculated, we cannot do partitioning by using the surface normal similarity.

4. Constrained Spectral Clustering

The proposed CSC is a constrained extension of SC. In this section, we first review SC briefly. Then, we propose CSC by utilizing the multiple similarities discussed previously, and derived an optimization algorithm for CSC based on eigen-decomposition.

4.1. Spectral Clustering (SC)

SC has been one of the modern clustering algorithms that are well studied in recent years(Shi and Jitendra, 1997; von Luxburg, 2006; Zelnik-Manor and Perona, 2004; Ng et al., 2001; Luxburg et al., 2004; Maila and Shi, 2001). By constructing an undirected weighted graph on the data, SC utilizes the spectrum of the graph Laplacian(Grone and Merris, 1994) to obtain a low dimensional representation of the data and then does clustering by using classical methods, such as k-means. Suppose the constructed graph is G(V,E, W), where V denotes the set of vertices, E is the set of edges, and W is the associated affinity matrix, i.e., the weights on the edges. The degree matrix D of graph G is a diagonal matrix, with entry $D_{ii} = \sum_{j=1}^{N} W_{ij}$. Then the graph Laplacian of G is defined(Grone and Merris, 1994) by

$$L = D - W \tag{5}$$

Further, in practice, one usually uses the so called normalized graph Laplacian(Luxburg et al., 2004) given by

$$\tilde{L} = D^{-1/2}LD^{-1/2} = I - D^{-1/2}WD^{-1/2} \tag{6}$$

The following theorem reveals a fundamental property of $\tilde{L}$, which also explains why $\tilde{L}$ can be used for performing clustering.

Theorem 1. *If graph G is an undirected with non-negative weights, then the multiplicity k of the eigenvalue 0 of $\tilde{L}$ equals to the number of connected components (subgraphs), G_1, ,G_k of G. Further, the eigenspace of 0 is spanned by the indicator vectors of the connected components multiplied by the square root of the degree matrix of G, i.e., $D^{1/2}1(G_i)$.*

According to Theorem 1, the connected components of G can be revealed by the optimization problem below,

$$\begin{aligned} \min_{H \in R^{N \times k}} \quad & tr(H^T LH) \\ s.t. \quad & H^T DH = I \end{aligned} \tag{7}$$

Because the columns of the optimal solution H^* just span the eigenspace of $\tilde{L}$ associated with eigenvalue 0. In practice, however, when we want to do k-partitioning of the data, the graph G constructed from the data does not necessarily have k connected components. Thus, we cannot directly find clusters from H^*. To this end, SC further conducts k-means clustering on H^* so as to obtain a clustering result.

4.2. Constrained Spectral Clustering (CSC)

To deal with multiple similarities, i.e., the distance similarity and the surface normal similarity, we extend SC to CSC by introducing constraints. According to the definition of surface normal similarity (4), if $S(i, j) = 1$, then x_i and x_j are close to each other and have similar surface normal. So x_i and x_j must belong to the same cluster. From SC, each h_m from H is an indicator vector, namely, $h_{i,m}$ and $h_{j,m}$, corresponding to x_i and x_j, have the same value. This simply encodes the surface normal similarity into algorithm SC. And the equation

$$\|h_{i,m} - h_{j,m}\| = 0, \quad m = 1, ..., k \tag{8}$$

is established. Equivalently,

$$\|h_{i,m} - h_{j,m}\|_2 = 0, \quad m = 1, ..., k \tag{9}$$

Equation (9) is in the quadratic form. Let Q^{ij} is a $N \times N$ symmetrical matrix and its entries are the coefficient of the quadratic form (9). So, the entries $[Q_{ii}^{ij} \;\; Q_{jj}^{ij} \;\; Q_{ij}^{ij} \;\; Q_{ji}^{ij}]$ are $[1 \;\; 1 \;\; -1 \;\; -1]$ while the remaining entries are filled with 0. Then, (9) can be rewritten as

$$h_m^T Q^{ij} h_m = 0, \quad m = 1, ..., k \tag{10}$$

Similarly, for other pairs points in $\tilde{V}$, the same conclusion can be obtained. For every pair surface normal similarity, we can simply add separate Q^{ij} together to obtain a synthetical matrix Q. Namely,

$$Q = \sum_{\substack{x_i \in \tilde{V} \\ y_i \in \tilde{V}}} Q^{ij} \tag{11}$$

For (11) is just a linear algebra, all surface normal similarities in $\tilde{V}$ can be written in one expression,

$$h_m^T Q h_m = 0, \quad m = 1, ..., k \tag{12}$$

For matrix H consists of k indicator h_m as columns, (12) can be reformulated as

$$tr(H^T Q H) = 0 \tag{13}$$

Until now, equation (13) integrates all prior knowledge and it only places some limitations on original problem (7)'s solution space. So, taking (13) as a constraint condition for (7) is appropriate. Finally, the CSC problem's objective function is

$$\begin{array}{rll} & \min & tr(H^T L H) \\ (CSC) & s.t. & H^T D H = I \\ & & \mathrm{tr}(H^T Q H) = 0 \end{array} \tag{14}$$

4.3. Solve CSC problem

The CSC (14) is a nonconvex problem(Bertsekas and Bertsekas, 1999) due to both the quadratic constraints, $H^T D H = I$ and $tr(H^T Q H) = 0$, and thus is generally difficult to solve. Possible ways are to use Lagrange or semidefinite programming relaxation to obtain a convex problem that is easy to deal with(Wang and Davidson, 2010; Coleman et al., 2008; Yu and

Shi, 2004). However, the main drawback of such relaxation is that there is generally no guarantee for exact optimal solution. Besides, computationally, the solving of the relaxed convex problems is still inefficient.

Our method to solve (14) is based on the observation that, although the trace constraint $tr(H^TQH) = 0$ is nonconvex, it can be addressed by exploiting the null space of Q , given that Q is positive semidefinite. Then, the rest orthogonality constraint can be dealt with by eigen-decomposition. The following Theorem 2 summarizes the ideas above.

Theorem 2. *The CSC (14) is equivalent to the following orthogonally constrained trace minimization*

$$\begin{array}{rll} \widetilde{CSC} & min & tr(A^T\widetilde{\widetilde{L}}A) \\ & s.t. & A^TA = I \end{array} \tag{15}$$

with

$$\widetilde{\widetilde{L}} = U_\perp^T \tilde{L} U_\perp \tag{16}$$

where $U_\perp$ is the eigenspace associated with the 0 eigenvalue of $D^{-1/2}QD^{-1/2}$, and $\tilde{L}$ is the normalized graph Laplacian.

Proof. First, by introducing variable $Y = D^{1/2}H$, the CSC problem (14) can be transformed into the equivalent problem below:

$$\begin{array}{rl} \min & tr(Y^T\widetilde{L}Y) \\ s.t. & Y^TY = I \\ & tr(Y^T\widetilde{Q}Y) = 0 \end{array} \tag{17}$$

where $\widetilde{L} = D^{-1/2}LD^{-1/2}$ is the normalized graph Laplacian, and $\widetilde{Q} = D^{-1/2}QD^{-1/2}$. It is clearly that $\tilde{Q}$ is positive semidefinite, given Q is positive semidefinite. Thus, we can eigen-decompose $\tilde{Q}$,

$$\tilde{Q} = \sum_{i=1}^{N} \lambda_i u_i u_i^T, \ \lambda_1 \geq \cdots \geq \lambda_p = \cdots = \lambda_N = 0 \tag{18}$$

Letting $U_\perp = [u_p, ..., u_N]$ and $m = N - p + 1$, then for any $y \in R^N$, the positive semidefinite property of $\tilde{Q}$ gives rise to

$$y^T\tilde{Q}y = 0 \Leftrightarrow y = U_\perp a. \quad for\ some\ a \in R^m \tag{19}$$

Thus, the trace constraint $tr(Y^T\widetilde{Q}Y) = 0$ is equivalently to the linear representation:

$$Y = U_\perp A,\ for\ some\ A \in R^{N\times m} \tag{20}$$

By using (20), the minimization (17) with respect to Y can be transformed to an equivalent problem with respect to A,

$$\begin{array}{cc} \min & tr(A^T U_\perp^T \widetilde{L}\ U_\perp A) \\ s.t. & A^T U_\perp^T U_\perp A = I \end{array} \tag{21}$$

Finally, since $U_\perp^T U_\perp = I$, we have

$$\widetilde{CSC}\quad \begin{array}{cc} \min & tr(A^T U_\perp^T \widetilde{L} U_\perp A) \\ s.t. & A^T A = I \end{array} \tag{22}$$

This completes the proof. □

Suppose the optimal solution of (15) is A^*. Then, according to the proof above, the optimal solution of (14) is given by

$$H^* = D^{-1/2} U_\perp A^* \tag{23}$$

The procedures for solving (14) is summarized as Algorithm 1 below.

Algorithm 1 Constrained Spectral Clustering

Require:

graph Laplacian L;
degree of graph D;
threshold for zero β;
constraint matrix Q;
number of cluster k;

Ensure:

the optimal cluster indicator H^*;

1: $\widetilde{L} = D^{-1/2} L D^{-1/2}$; $\widetilde{Q} = D^{-1/2} Q D^{-1/2}$;
2: $[V\ \ lam] = SVD(\widetilde{Q})$;
3: $indx = find(diag(lam)\ <\ \beta)$;
4: $U_\perp = V(:, indx)$;
5: $[A\ \ Z] = SVD(U_\perp^{\mathrm{T}} \times \widetilde{L} \times U_\perp)$;
6: $A = A(:, end - k + 1 : end)$;
7: $Y = U_\perp \times A$;
8: $H = diag(D^{-1/2}) \times Y$;

5. Experimental Results

In this section, we conduct a set of experiments to validate our proposed algorithm's effectiveness.

The 3D human body point cloud used in our experiments are obtained by emulating human action sequences. Not only full-human body point cloud, but also semi-human body point cloud is emulated for considering the binocular cameras' applications. Some of these point cloud contains more than 5000 points, and some of them contains only more than 800 points. Obviously, the points we sample from human body is less than other literatures (Xiao et al., 2003). Considering segmentation results on these less points make our method capacity for real time applications. We choose frames consisted of point cloud from kinds of human action sequences, e.g. running, leg-lifting and sprint. Many unexpected situations can appear when one does these actions. when one raises his arms, lower arm may occludes upper arm. When one lifts one of his legs, the other leg supporting the body may standing too long to segment considerably by unconstraint method. Additionally, situation that two legs get close to each other or two arms are close to the torso is inevitable. For these behaviors are performed by various postures other than the standard pose (Xiao et al., 2003; Werghi and Xiao, 2002), we desire to show our method's ability. We evaluate the effectiveness of our algorithm in terms of quality of posture segmentation and superiority comparing to classical clustering way, e.g., k-means and standard SC.

Figure. 2 and 3 shows the full-human body point cloud segmentation results. These point cloud comprise approximate 5000 points. The plots from first to last column successively are original point cloud, segmentation result of k-means, segmentation result of SC, segmentation result of CSC.

Figure. 2 are two different frames of sprint action. As one knee bends, the point Euler distances between upper and low leg close to knee are smaller than their geodesic distance along with human body surface. Without question, k-means with Euler distance information cannot divide leg at knee into two parts. Meanwhile, as k-means always obtains size-alike groups, the large area of torso and the long unbend leg are segmented into several small parts. As some literature mention, SC always segments large area into several groups, and this reflects in the torso of our SC segmentation result. But, from the prior knowledge, the large flat torso should be grouped as one group. That's exactly our constraint condition does. Normals of Points that form torso are similar to each other. Around the center of torso, the points

normal placed as a circle. Encode this constraint into SC, we improve the quality of segmentation result as the plots show. From our CSC results, we can extract topologic features more reliable.

Figure. 3 are two various frames from leg-lifting behaviors. Besides the large flat torso and bend knee, another demanding place is the unbend leg. In Figure. 3(a), the leg has bended a little although almost directly straight, the little bended angle can be utilized and two line constraints alongside upper leg and lower leg separately are encoded in our CSC algorithm. The plot shows effectiveness of our approach. But Figure. 3(b), as the unbend leg is too straight to distinguish upper leg and lower leg with point normal. So, more other useful feature should be extracted to settle for this problem.

Figure. 4 and 5 shows the semi-human body point cloud segmentation results. These point cloud comprise only approximate 800 points. This set of results desires to explain our method's potential for real-time applications. Similarly with Figure. 2 and 3, the plots from first to last column successively are original point cloud, segmentation result of k-means, segmentation result of SC, segmentation result of CSC.

Figure. 4 are semi-human body point cloud from leg-lifting action. In Figure. 4(a), one of arms is absent for it is occluded by torso as one throws his arm back. The clustering for this situation can be solved with time sequence and this paper's attention is not here. As lifting lower leg, the upper leg is occluded partially. Although points on upper leg is much less, with their unique points normal comparing with normal of torso and lower leg, upper leg points are clustered as one cluster as segmentation result of CSC shows. In Figure. 4(b), this behavior happens when swapping lifting legs. The two lower legs are too close to divide them as two groups for k-means and SC. But, the points normal of two lower legs face different orientations. Again, normal information from surface of human body is encoded in our CSC method and helps to accomplish considering segmentation results.

Figure. 5 are semi-human body point cloud from running action sequences. Comparing above situations that are hard to segment, this action is much easy to cluster just except the large flat torso. And it easily group several small fractions of torso into one group with their similar point normal feature.

All above results show our method's effectiveness and point normal feature's rationality.

6. Conclusions

In this paper, we achieved the task of automatically segmenting 3D human posture formed by point cloud by using our proposed CSC method. We use local feature - distance similarity and graph Laplacian to keep the manifold on which 3D data points scatter while we additionally utilize human body surface normal similarity as constraint to original SC to address the limitations of it and enhance the segmenting results. We showed the effectiveness of our method and also showed the advantage of our approach over k-means and SC.In the future, the segmentation results will be used as a building base block for following-up human action analysis.

References

Bertsekas, D. P., Bertsekas, D. P., September 1999. Nonlinear programming. 2nd Edition. Athena Scientific.
URL http://www.worldcat.org/isbn/1886529000

C.C.L, W., T.K.K, C., M.M.F., Y., 2003. From laser-scanned data to feature human model: a system based on fuzzy logic concept. Vol. 35. pp. 241–253.

Chen, C.-C., Hsieh, J.-W., Hsu, Y.-T., Huang, C.-Y., 2006. Segmentation of human body parts using deformable triangulation. Vol. 1. IEEE Computer Society, pp. 355–358.

Coleman, T., Saunderson, J., Wirth, A., 2008. Spectral clustering with inconsistent advice. In: ICML '08: Proceedings of the 25th international conference on Machine learning. ACM, New York, NY, USA, pp. 152–159.

Dekker, L., Douros, I., Buxton, B., Treleaven, P., 1999. Building symbolic information for 3d human body modeling from range data. Vol. 0. IEEE Computer Society, Los Alamitos, CA, USA, p. 0388.

Grone, R., Merris, R., 1994. The laplacian spectrum of a graph ii. Vol. 7. Society for Industrial and Applied Mathematics, Philadelphia, PA, USA, pp. 221–229.

hsuan Yang, M., Ahuja, N., 1999. Gaussian mixture model for human skin color and its applications in image and video databases. In: Its Application in Image and Video Databases. Proceedings of SPIE 99 (San Jose CA. pp. 458–466.

Jagannathan, A., 2005. segmentation and recognition of 3d point clouds within graph-theoretic and thermodynamic frameworks.

Ju, X., Werghi, N., Siebert, J. P., 2000. Automatic segmentation of 3d human body scans. In: Proc. IASTED Int. Conf. on Computer Graphics and Imaging 2000 (CGIM 2000), Las Vegas. pp. 239–244.

Kannan, R., Vempala, S., Vetta, A., 2000. On clusterings: Good, bad and spectral.

Kanungo, T., Mount, D. M., Netanyahu, N. S., Piatko, C. D., Silverman, R., Wu, A. Y., 2002. An efficient k-means clustering algorithm: Analysis and implementation. Vol. 24. IEEE Computer Society, Washington, DC, USA, pp. 881–892.

K.H., W. H. K. E. W. S. L., 2002. A new segmentation method for point cloud data. Vol. 42. pp. 167–178.

Luxburg, U. V., Bousquet, O., Belkin, M., 2004. Limits of spectral clustering. MIT Press, pp. 857–864.

Maila, M., Shi, J., 2001. A random walks view of spectral segmentation. In: AI and STATISTICS (AISTATS) 2001.

Mori, G., Ren, X., Efros, A. A., Malik, J., 2004. Recovering human body configurations: Combining segmentation and recognition. Vol. 2. pp. 326–333.

Ng, A. Y., Jordan, M. I., Weiss, Y., 2001. On spectral clustering: Analysis and an algorithm. In: Dietterich, T. G., Becker, S., Ghahramani, Z. (Eds.), Advances in Neural Information Processing Systems. Vol. 14.

Nurre, J. H., 1997. Locating landmarks on human body scan data. In: NRC '97: Proceedings of the International Conference on Recent Advances in 3-D Digital Imaging and Modeling. IEEE Computer Society, Washington, DC, USA, p. 289.

Shi, J., Jitendra, M., 1997. Normalized cuts and image segmentation.

Song, Y., Goncalves, L., Perona, P., 2003. Unsupervised learning of human motion. Vol. 25. pp. 814–827.

von Luxburg, U., 2006. A tutorial on spectral clustering.

Wang, X., Davidson, I., 2010. Flexible constrained spectral clustering. In: KDD '10: Proceedings of the 16th ACM SIGKDD international conference on Knowledge discovery and data mining. ACM, New York, NY, USA, pp. 563–572.

Weik, Sebastian, Liedtke, Claus-E., 2001. Hierarchical 3d pose estimation for articulated human body models from a sequence of volume data. In: RobVis '01: Proceedings of the International Workshop on Robot Vision. pp. 27–34.

Werghi, N., Xiao, Y., 2002. Recognition of human body posture from a cloud of 3d points using wavelet transform coefficients. In: In Proc. of the fifth IEEE International Conference on Automatic face and gesture recognition.

Xiao, Y., Siebert, P., Werghi, N., 2003. A discrete reeb graph approach for the segmentation of human body scans. Vol. 0. IEEE Computer Society, Los Alamitos, CA, USA, p. 378.

Yilmaz, A., Javed, O., Shah, M., 2006. Object tracking: A survey. Vol. 38. ACM, New York, NY, USA, p. 13.

Yu, S. X., Shi, J., 2004. Segmentation given partial grouping constraints. Vol. 26. IEEE Computer Society, Washington, DC, USA, pp. 173–183.

Zelnik-Manor, L., Perona, P., 2004. Self-tuning spectral clustering. In: Advances in Neural Information Processing Systems. Vol. 17. MIT Press, pp. 1601–1608.
URL http://citeseerx.ist.psu.edu/viewdoc/summary?doi=10.1.1.84.7940

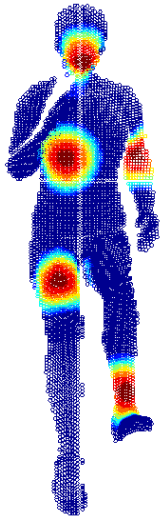

(a)

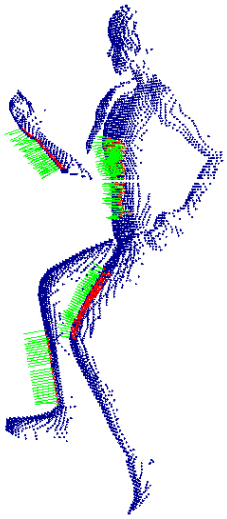

(b)

Figure 1: distance similarity and surface normal similarity

(a)

(b)

Figure 2: Segmentation results of sprint posture formed by full-human body point cloud with respect to method variations

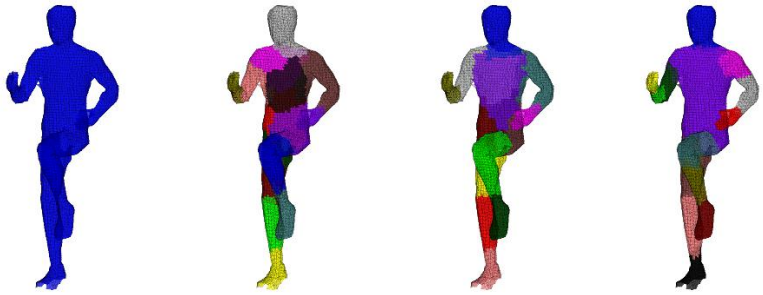

(a)

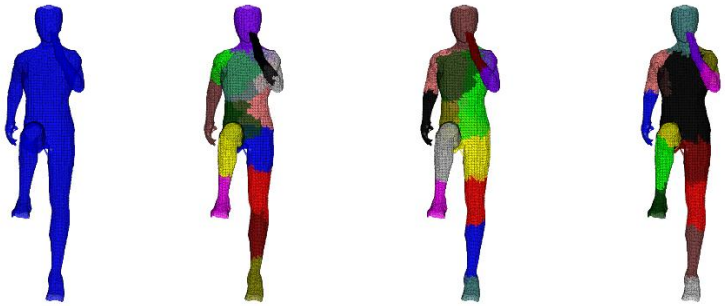

(b)

Figure 3: Segmentation results of leg-lifting posture formed by full-human body point cloud with respect to method variations

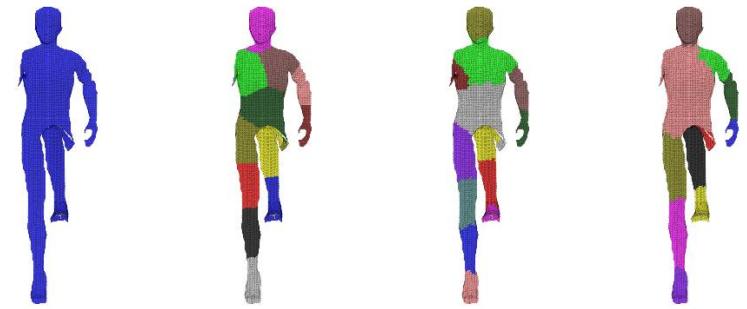

(a)

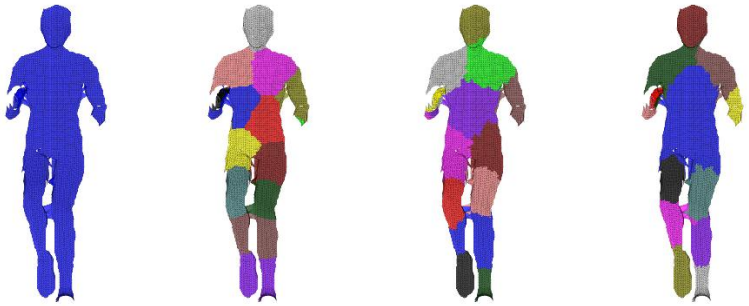

(b)

Figure 4: Segmentation results of leg-lifting posture formed by semi-human body point cloud with respect to method variations

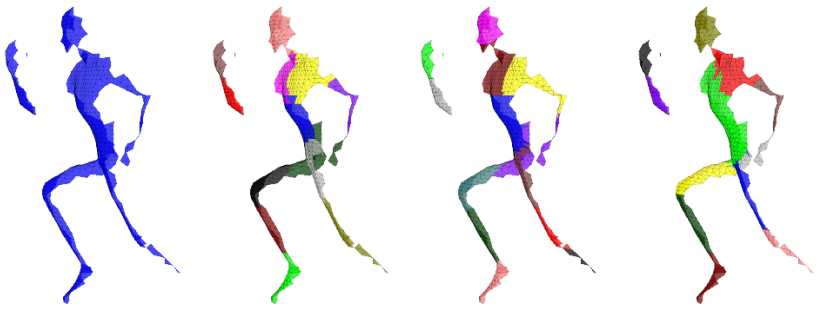

(a)

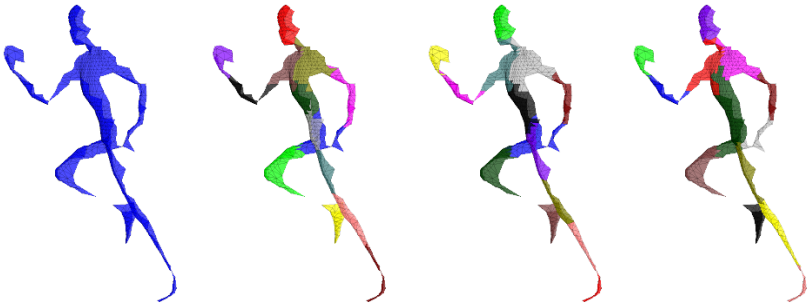

(b)

Figure 5: segmentation results of running posture formed by semi-human body point cloud with respect to method variations